JACS
JOURNAL OF THE AMERICAN CHEMICAL SOCIETY
Article
pubs.acs.org/JACS

Tuning the Electromechanical Properties of Single DNA Molecular Junctions

Christopher Bruot, Limin Xiang, Julio L. Palma, Yueqi Li, and Nongjian Tao*

Center for Bioelectronics and Biosensors, Biodesign Institute School of Electrical, Computer and Energy Engineering, Arizona State University, Tempe, Arizona 85287-5801, United States

Supporting Information

ABSTRACT: Understanding the interplay between the electrical and mechanical properties of DNA molecules is important for the design and characterization of molecular electronic devices, as well as understanding the role of charge transport in biological functions. However, to date, force-induced melting has limited our ability to investigate the response of DNA molecular conductance to stretching. Here we present a new molecule−electrode linker based on a hairpin-like design, which prevents force-induced melting at the end of single DNA molecules during stretching by stretching both strands of the duplex evenly. We find that the new linker group gives larger conductance than previously measured DNA−electrode linkers, which attach to the end of one strand of the duplex. In addition to changing the conductance the new linker also stabilizes the molecule during stretching, increasing the length a single DNA molecule can be stretched before an abrupt decrease in conductance. Fitting these electromechanical properties to a spring model, we show that distortion is more evenly distributed across the single DNA molecule during stretching, and thus the electromechanical effects of the $\pi-\pi$ coupling between neighboring bases is measured.

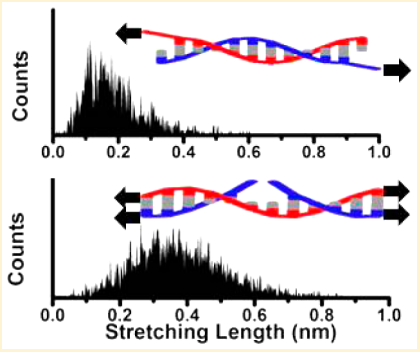

INTRODUCTION

In single molecule electronic devices, where single molecules are suspended between two metal electrodes, the electronic response is often coupled to the mechanical properties of the device.[1−3] This gives rise to the electromechanical response of the molecular junction, i.e., the change in conductance with a mechanical force applied to the molecule. Typically the electromechanical response of molecular junctions is determined by the response of the electrodes or change in the molecule−electrode coupling, because the metal electrodes (e.g., Au) have much softer bonds than the molecule.[4−8] Thus, to date, few studies have investigated the response of molecular conductance to the mechanically induced changes in the molecule. One candidate molecule to study truly molecular electromechanical properties is DNA, which transports charge through a thermally activated hopping process mediated by the $\pi-\pi$ interaction between neighboring bases.[9−13] Applying a mechanical force on single DNA molecules causes a structural transition away from native B-form of DNA, which should lead to intrinsic electromechanical properties in single molecule DNA experiments.[14−17] However, for short DNA molecules (~10 base pairs) this transition is caused by force-induced melting of the base pairs of the duplex DNA.[16,18,19] Recent single molecule transport experiments showed that this denaturing process has dramatic implications for the evolution of charge transport in single DNA molecular junctions.[11,20,21] Using the scanning tunneling microscope (STM) break junction technique, it was demonstrated that there is a sudden decrease in conductance associated with force-induced melting at short stretching lengths for DNA molecules stretched from the 3′ ends of complementary strands. Following de Gennes' model[16,17,22,23] for the mechanical properties of DNA, these short stretching lengths were attributed to force-induced breaking of the end base pairs causing a sudden change in the coupling between DNA and electrode. These experiments show that the mechanical properties of the DNA molecule play a large role in the evolution of charge transport in molecular junctions. Still, force-induced melting of the end base pairs prohibits a deeper understanding of the role of $\pi-\pi$ coupling between neighboring bases and the electromechanical properties of DNA.

Here we present a new design of single DNA molecule contact which exploits a hairpin-like "closed-end" DNA structure to overcome the force-induced melting of the end base pairs. Utilizing the STM break junction technique in native aqueous environment, we compare the molecular conductance and stretching length properties of the new closed-end DNA design to the more traditional free-end DNA. We find that, while the transport mechanism is thermally activated hopping for both contact schemes, the molecule−electrode coupling is larger for closed-end DNA resulting in larger molecular conductance. Additionally, comparing the stretching length of closed-end DNA and free-end DNA we show that stretching both strands evenly, as is the case for closed-end DNA, results in significantly larger stretching lengths compared to stretching

Received: August 26, 2015
Published: October 19, 2015

DOI: 10.1021/jacs.5b08668
J. Am. Chem. Soc. 2015, 137, 13933−13937

individual strands of the double-helix. Furthermore, closed-end DNA demonstrates stretching length dependence on molecular length, a signature of stretching the DNA molecule instead of breaking end base pairs. Using a spring-ladder model, similar to that of de Gennes, we describe the stretching of closed-end DNA as being distributed across the molecule more evenly and extract the relative importance of all portions of the DNA molecule.

EXPERIMENTAL PROCEDURE

In order to stabilize the end base pairs, a DNA hairpin structure was designed such that the linker group is equally bound to both strands after hybridizing. To achieve the hairpin-like structure, the linker consists of a thiol-modified thymine base (thiol-T) between two alkane spacers (three carbon), where the thiol groups can bind with gold electrodes to form a molecular junction. Synthesized into a single strand of DNA, this linker group is designed to provide a point for the molecule to bend and the bases on either side to hybridize creating a hairpin with the thiol-T free, as can be seen from the native electrophoresis gel (Figure S1). The structure of the closed-end DNA linker can be seen in Figure 1a. Inserting two of these linker groups

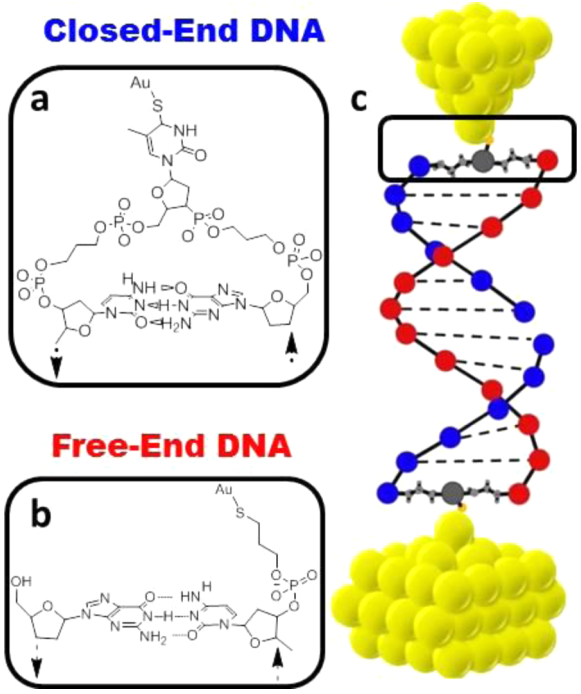

Figure 1. Closed-end vs free-end DNA. (a) Chemical structure of the closed-end DNA linker group. (b) Chemical structure the free-end DNA linker group. (c) Illustration of a single DNA molecular junction.

into an appropriate sequence of single strand DNA allows the single strand to fold upon itself and hybridize into double strand DNA. In this report, closed-end DNA molecules follow the sequence 5′-C_NG-linker-CG_{2xN}C-linker-GC_N-3′, where N = 4, 6, 8, and 10. The resulting structure is native B-form DNA, as shown by polyacrylamide gel electrophoresis (PAGE), circular dichroism (CD) spectroscopy and melting temperature measurements in the Supporting Information, with a closed-end linker group at each end. It should be noted that the position where the 5′ and 3′ ends meet is similar to a "nick site" which is created by phosphodiester bond hydrolysis, although there is no such reaction occurring in the present experiments. For comparison, the free-end linker group, Figure 1b, consists of a thiol linker group attached to the 3′ (5′) end of a single strand through a three (six) carbon spacer.[24] Here, we studied free-end DNA with thiol linkers in the 3′−3′, 5′−5′, and 5′−3′ configurations, the first two having linker groups on opposite strands and the last having thiol linkers on each end of a single strand within the duplex.

The STM break junction technique was used to measure the resistance and stretching length of DNA molecules with free-end and closed-end linkers described above. This method to measure charge transport in single molecules has been detailed elsewhere.[25−27] Briefly, phosphate buffer solution containing the DNA molecule of interest is pipetted onto the gold STM substrate, such that the molecules form gold−thiol bonds with the surface. An atomically sharp gold STM tip is brought into contact with the substrate, to create a gold bridge, than retracted from the surface. Absent a molecule, an applied bias between tip and substrate creates a tunneling current, which decreases exponentially with tip retraction, black traces in Figure 2a. In the

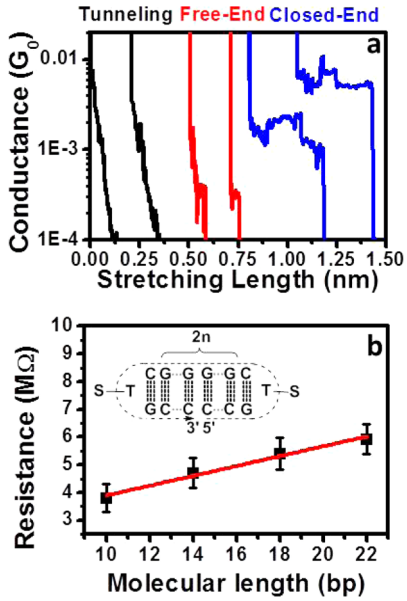

Figure 2. Transport characteristics of closed-end DNA (a) Conductance vs stretching length traces for tunneling through solvent (black traces), transport through free-end DNA (red traces) and transport through closed-end DNA (blue traces). (b) Resistance vs molecular length for closed-end DNA molecules ranging from 10 to 22 base pairs in length. Inset illustrates the structure and sequence of closed-end DNA. Error bars depict the standard error of the mean between at least n = 4 experiments. Red line is linear fitting of resistance data from which the slope and intercept are determined.

presence of molecules, plateaus can be seen in the current vs tip retraction trace. These plateaus represent single molecules bridging the tip−substrate gap, red and blue traces in Figure 2a. The distance the tip retracts during the final plateau, before the current abruptly drops to zero, is considered the stretching length. This break junction process is repeated thousands of times for each molecule studied, compiling the conductance traces into a conductance histogram in order to determine the statistically most probable conductance of a single molecule. Likewise, the stretching lengths of each molecular junction are compiled into a stretching length histogram, which gives the most probable stretching length for the molecules studied. In this report, all cited resistance (inverse of conductance) and stretching length values are the average of at least 4 separate experiments and all error bars are the standard error of the mean.

RESULTS

The single molecule resistance (inverse of conductance) of closed-end DNA is linearly dependent on molecular length, Figure 2b, indicating that the predominant transport mechanism in closed-end DNA is thermally activated hopping. This is in good agreement with previous transport measurements for

DOI: 10.1021/jacs.5b08668
J. Am. Chem. Soc. 2015, 137, 13933−13937

DNA molecules more than a few bases long. In the hopping regime, transport is mediated by transport through the nucleic acid base with the lowest ionization energy, typically guanine. Following the model proposed by Nitzan[28,29] for hopping transport in DNA, resistance as a function of number of hopping sites (N) can be expressed as

$$R \propto \frac{1}{k_L} + \frac{1}{k_R} + \frac{(N-1)}{k} \quad (1)$$

Here, $k_{L(R)}$ are the charge transfer rate between the first hopping site and the left (right) electrodes, and k is the charge transfer rate between neighboring hopping sites within the DNA molecule. The term which is omitted for clarity in eq 1 depends on the activation energy for hopping processes, and is unknown in the case for charge transport in single DNA molecular junctions.[30] A linear fitting of resistance to length, however, allows us to determine the relative importance of transport across the molecule−electrode contact and among neighboring hopping sites through the ratio of the slope and intercept. For closed-end DNA, we find a ratio of approximately 13, meaning that transport between neighboring bases is ∼13 times faster than that at the contacts. Compared to the ratio of free-end DNA of 40,[20] reported previously, we find that the relative importance of the contact resistance of closed-end DNA is smaller than that of free-end DNA. This is further demonstrated by evaluating the measured resistance of closed-end and free-end DNA of similar length, Table 1. Closed-end DNA has consistently smaller resistance, i.e., is more conductive, than free-end DNA indicating that the type of linker plays a large role in the absolute value of resistance for DNA charge transport. In addition, it should be noted that free-end linkers which contain 5′ terminated thiols (5′−5′ and 3′−5′) have larger values of resistance, most likely due to the six carbon bonds between the thiol and first guanine hopping site as opposed to three for the 3′ linker.

Table 1. Measured Resistance and Stretching Length for the Different Linkers Studied in This Report[a]

linker	resistance (MΩ)	stretching length (nm)
closed-end	3.8 ± 0.5	0.37 ± 0.04
3′−3′	12.5 ± 2.2	0.12 ± 0.01
5′−5′	27.4 ± 1.8	0.13 ± 0.01
3′−5′	41.6 ± 3.5	0.16 ± 0.02

[a]Error values correspond to the standard error of the mean of at least n = 4 experiments.

In addition to decreasing the molecular resistance, DNA with closed-end linker groups also have longer stretching lengths than free-end DNA. Figure 3 illustrates this by showing stretching length histograms of free-end and closed-end DNA molecules of the same length, 10 base pairs (∼3 nm). As we can see, the stretching length of free-end DNA is constant, independent of linker geometry, around 0.12−0.16 nm. This is in good agreement with previously reported measurements of stretching length for 3′−3′ free-end DNA of lengths from 6 to 26 base pairs.[20] As discussed above, this relatively small stretching length, only a few percent of molecular contour length, is a signature of force-induced breaking of the end base pairs. On the other hand, 10 base pair closed-end DNA has a stretching length of ∼0.37 nm, nearly double that of free-end. This indicates that the hairpin structure of closed-end DNA is affecting the mechanical process involved in abrupt decrease in current which corresponds to the stretching length. In other words, the increased stretching length suggests that closed-end DNA does not undergo force-induced melting in the same way as free-end DNA.

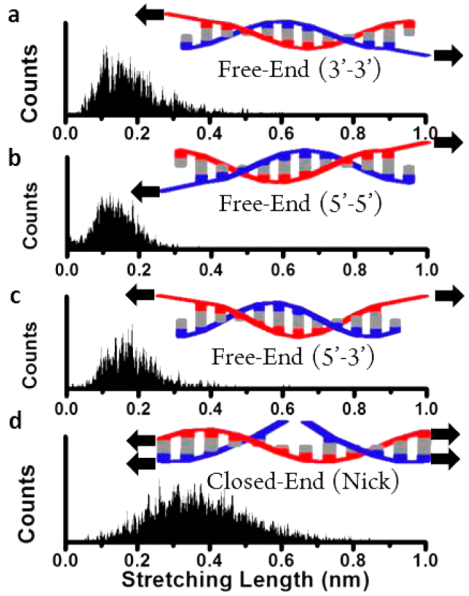

Figure 3. Mechanical characteristics of different DNA linkers. Stretching length histograms for 10 base pair DNA molecules contacted to the molecule at the (a) 3′−3′, (b) 5′−5′, or (c) 5′−3′ ends and the closed-end DNA linker (d). Insets illustrate which strands are stretched and the most probable breaking mechanism.

The stretching length of closed-end DNA is also more strongly dependent on molecular length than free-end DNA. As was reported previously, free-end DNA is weakly dependent on DNA molecular length for lengths ranging from 6 to 26 base pairs,[20] Figure 4b. This was attributed to the breaking of the end base pairs under mechanical force due to the uneven distribution of strain within de Gennes' model for stretching DNA. However, the stretching length of closed-end DNA increases with molecular length from 0.37 to 0.52 nm for 10 to 22 base pairs, respectively. In addition, the stretching length of closed-end DNA increases linearly with number of base pairs, as can be seen in Figure 4b. The observation of a linear increase of stretching length with molecular length is in sharp disagreement with de Gennes' model for the mechanical properties of DNA stretched from single strands, i.e., free-end structure, which predicts weak length dependence. Along with the overall increase in stretching length, this indicates that the mechanism behind the abrupt decrease in current, which determines the stretching length, is different from the force-induced melting of end base pairs predicted for free-end DNA by de Gennes' model.[17]

DISCUSSION

To explain the linear increase in stretching length with molecular length observed for closed-end DNA, we present a model for stretching closed-end DNA which approximates the interaction between neighboring bases as simple harmonic springs. This model is illustrated in Figure 4a. The closed-end DNA molecular junction is modeled by springs with four different spring constants: those representing the Au−Au bonds (k_{Au}), those representing the neighboring bases which are located where the 3′ and 5′ ends of the original DNA single

DOI: 10.1021/jacs.5b08668
J. Am. Chem. Soc. 2015, 137, 13933−13937

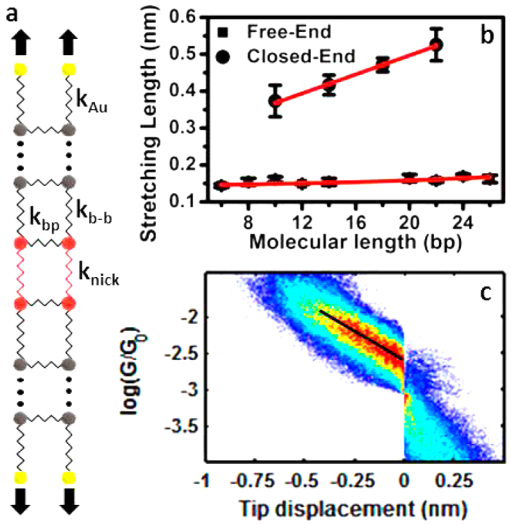

Figure 4. Electromechanical properties of closed-end DNA. (a) Spring system used to model closed-end DNA as two series of springs in parallel. Each side consists of the gold-DNA bonds, base−base interaction and base−base interaction at the nick site. (b) Stretching length dependence on molecular length for both closed-end (circles) and free-end (squares) DNA. Error bars depict the standard error of the mean between at least $n = 4$ experiments. Red lines show fitting of stretching length to eq 2 and de Gennes' model for closed-end and free-end DNA, respectively. A more detailed plot showing the fitting for closed-end DNA is shown in the Supporting Information. (c) 2-Dimensional histogram of logarithm of conductance vs stretching length for 14 base pair closed-end DNA. Black line is a guide for the eye demonstrating the slope of conductance vs stretching length, which is the electromechanical response of closed-end DNA.

strand meet (the "nick site") (k_{nick}), those representing the interaction between all other neighboring base pairs (k_{b-b}), and those representing the base pairing interaction between hydrogen bonded bases (k_{bp}). Here we make a distinction between the spring constant at the site where the 5′ and 3′ ends meet and for the other neighboring base pairs because the "nick site" is missing phosphodiester bonds in the backbone, only relying on the $\pi-\pi$ interaction between adjacent bases for structure. Since the mechanical force is presumably evenly distributed between both strands of hybridized closed-end DNA, we can ignore the hydrogen bonding spring interaction. Thus, using Hooke's law, we can express the stretching length (X) of closed-end DNA, as a function of the force applied to the molecular junction when the abrupt decrease in current occurs ($F_{breakdown}$) and the equivalent spring constant for the molecular junction, as

$$X = F_{breakdown}\left[\frac{1}{k_{Au}} + \frac{1}{2k_{nick}} + \frac{N-2}{2k_{b-b}}\right] \quad (2)$$

From previous experiments we know that $k_{Au} = 8$ N/m[31,32] and $k_{b-b} = 2.6$ N/m per base pair.[33] Using these parameters, fitting the measured stretching length results in $k_{nick} = 0.13 \pm 0.009$ N/m per base pair and $F_{breakdown} = 67 \pm 2.8$ pN.

One striking result of this model is that the force required to achieve abrupt decrease in current is equal to that for the so-called B−S transition, in which DNA is stretched out of native B-form. Force spectroscopy measurements have shown that this transition occurs around 65−70 pN.[14,15,19] This is opposite to what was found for free-end DNA, in which the breakdown force is much smaller. A similar change in mechanical response of DNA was seen in the force spectroscopy measurements of Paik et al.,[19] in which they show that topologically closed DNA sequences do not display hysteresis in force−extension curves, a signature of force-induced melting. Furthermore, Paik et al. show that introduction of a nick site to the DNA sequence allows for force-induced melting to be localized to the nick site, the weakest point in the DNA molecule. Similar to the work of Paik et al., the present model indicates that the nick site has a much smaller spring constant than normally neighboring base pairs. This indicates that as the closed-end DNA molecule is stretched, a larger portion of the mechanical strain is distributed between the neighboring base pairs at the nick site than the other sites. From the fitting, we can see that the nick site is stretched by ∼0.25 nm before the abrupt decrease in current. Comparatively, the Au−Au bonds of the electrodes are stretched just ∼0.008 nm. The remaining stretching length for each molecule is distributed evenly among the rest of the base pairs, resulting in the observed molecular length dependence.

Having shown that the stretching length characteristics of closed-end DNA molecular junctions are determined by the mechanical properties of the molecule and not the electrodes or coupling between the molecule and electrodes, we now turn our attention to the electromechanical response of closed-end DNA. The simplest method of extracting information on the electromechanical response of a single molecule junction is to determine the response of conductance to electrode separation. This is achieved by extracting the slope of conductance vs tip displacement. In the case of a tunneling junction, this slope is proportional to the height of the tunneling barrier. Similarly, in closed-end DNA molecular junctions this slope represents the decay of the $\pi-\pi$ interaction between neighboring base pairs, particularly the base pairs surrounding the nick site where most of the distortion takes place. To extract the conductance vs tip displacement slope we compile the traces into a 2-dimensional histogram of logarithm of conductance vs tip displacement, aligning all traces on the tip retraction axis so that zero tip displacement is the point where the current abruptly drops to zero. Figure 4C shows the 2D conductance vs tip displacement histograms for the closed-end DNA 14 base pairs in length. The peak conductance values at each tip displacement along the plateau are then extracted by Gaussian fitting and the slope versus stretching length is extracted. For all closed-end DNA samples measured this slope is approximately 3 nm^{-1}, see Table S1 for exact values. These values are similar to the decay constant of other π orbital coupling systems, particularly the interaction between π orbitals and gold surfaces.[7,34] In addition, this value is in agreement with the decay constant between neighboring guanine bases measured through tip modulation.[35]

CONCLUSIONS

In summary we demonstrate a novel molecule−electrode linker scheme for single DNA molecule electronics that overcomes the mechanical limitations of free-ended double helix DNA. This closed-end DNA has a larger conductance than free-end DNA of similar length, which can be attributed to stronger molecule−electrode coupling. Closed-end DNA also exhibits unique mechanical properties, measured through the stretching length in STM break junction experiments. In addition to substantially longer stretching lengths, closed-end DNA is also more strongly dependent on molecular length. Utilizing a model which approximates DNA as a linear network of springs, we show that these mechanical properties are a product of the

DOI: 10.1021/jacs.5b08668
J. Am. Chem. Soc. 2015, 137, 13933−13937

stretching force being more evenly distributed along the molecular junction for closed-end DNA, as opposed to free-end DNA in which the end base pairs have been shown to melt. Further, we show that the abrupt decrease in current during STM break junction experiments with closed-end DNA is a product of force-induced melting at the weakest point along the strand, the nick site. Finally, the response of conductance to stretching is investigated and is correlated to the change in conductance expected for π coupled systems. These unique electrical and mechanical characteristics of closed-end DNA make this molecular structure an intriguing candidate for further investigating the electromechanical properties of DNA and for the development of molecular electromechanical devices from DNA.

■ ASSOCIATED CONTENT

Supporting Information

The Supporting Information is available free of charge on the ACS Publications website at DOI: 10.1021/jacs.5b08668.

Experimental methods, DNA characterization data, and electromechanical data. (PDF)

■ AUTHOR INFORMATION

Corresponding Author

*njtao@asu.edu

Notes

The authors declare no competing financial interest.

■ ACKNOWLEDGMENTS

The authors would like to thank Dr. Arunoday Singh and Prof. Fredrick D. Lewis for helpful discussions regarding the closed-end DNA structure, Angela D. Edwards for help performing and deciphering PAGE experiments, and ONR(N00014-11-1-0729) for financial support.

■ REFERENCES

(1) Xu, B. Q.; Li, X. L.; Xiao, X. Y.; Sakaguchi, H.; Tao, N. J. *Nano Lett.* **2005**, *5* (7), 1491.
(2) Nacci, C.; Fölsch, S.; Zenichowski, K.; Dokić, J.; Klamroth, T.; Saalfrank, P. *Nano Lett.* **2009**, *9* (8), 2996.
(3) Parks, J. J.; Champagne, A. R.; Costi, T. A.; Shum, W. W.; Pasupathy, N.; Neuscamman, E.; Flores-Torres, S.; Cornaglia, P. S.; Aligia, A. A.; Balseiro, C. A.; Chan, G. K.-L.; Abruña, H. D.; Ralph, D. C. *Science* **2010**, *328* (5984), 1370.
(4) Bruot, C.; Hihath, J.; Tao, N. *Nat. Nanotechnol.* **2012**, *7* (1), 35.
(5) Perrin, M. L.; Verzijl, C. J. O.; Martin, C. a.; Shaikh, A. J.; Eelkema, R.; van Esch, J. H.; van Ruitenbeek, J. M.; Thijssen, J. M.; van der Zant, H. S. J.; Dulić, D. *Nat. Nanotechnol.* **2013**, *8*, 282.
(6) Aradhya, S. V.; Frei, M.; Hybertsen, M. S.; Venkataraman, L. *Nat. Mater.* **2012**, *11* (10), 872.
(7) Diez-Perez, I.; Hihath, J.; Hines, T.; Wang, Z.-S.; Zhou, G.; Müllen, K.; Tao, N. *Nat. Nanotechnol.* **2011**, *6* (4), 226.
(8) Meisner, J. S.; Kamenetska, M.; Krikorian, M.; Steigerwald, M. L.; Venkataraman, L.; Nuckolls, C. *Nano Lett.* **2011**, *11* (4), 1575.
(9) Xu, B.; Zhang, P.; Li, X.; Tao, N. *Nano Lett.* **2004**, *4* (6), 1105.
(10) Giese, B.; Amaudrut, J.; Kohler, A.; Spormann, M.; Wessely, S. *Nature* **2001**, *412* (May), 318.
(11) Song, B.; Elstner, M.; Cuniberti, G. *Nano Lett.* **2008**, *8* (10), 3217.
(12) Voityuk, A.; Jortner, J.; Bixon, M.; Rösch, N. *J. Chem. Phys.* **2001**, *114* (13), 5614.
(13) Xiang, L.; Palma, J. L.; Bruot, C.; Mujica, V.; Ratner, M. A.; Tao, N. *Nat. Chem.* **2015**, *7* (3), 221.
(14) Smith, S. B. S.; Cui, Y.; Bustamante, C. *Science* **1996**, *271* (5250), 795.
(15) Cluzel, P.; Lebrun, A.; Heller, C. *Science* **1996**, *271* (5250), 792.
(16) Hatch, K.; Danilowicz, C.; Coljee, V.; Prentiss, M. *Phys. Rev. E* **2008**, *78* (1), 011920.
(17) De Gennes, P.-G. *C. R. Acad. Sci., Ser. IV: Phys., Astrophys.* **2001**, *2* (10), 1505.
(18) Rouzina, I.; Bloomfield, V. a. *Biophys. J.* **2001**, *80* (2), 882.
(19) Paik, D. H.; Perkins, T. T. *J. Am. Chem. Soc.* **2011**, *133* (10), 3219.
(20) Bruot, C.; Xiang, L.; Palma, J. L.; Tao, N. *ACS Nano* **2015**, *9* (1), 88.
(21) Kang, N.; Erbe, a; Scheer, E. *New J. Phys.* **2008**, *10* (2), 023030.
(22) Nath, S.; Modi, T.; Mishra, R. K.; Giri, D.; Mandal, B. P.; Kumar, S. *J. Chem. Phys.* **2013**, *139* (16), 165101.
(23) Wolter, M.; Woiczikowski, P. B.; Elstner, M.; Kubař, T. *Phys. Rev. B: Condens. Matter Mater. Phys.* **2012**, *85* (7), 075101.
(24) Hihath, J.; Chen, F.; Zhang, P.; Tao, N. *J. Phys.: Condens. Matter* **2007**, *19* (21), 215202.
(25) Xu, B.; Tao, N. J. *Science* **2003**, *301* (5637), 1221.
(26) Tao, N. J. *Nat. Nanotechnol.* **2006**, *1*, 173.
(27) Guo, S.; Hihath, J.; Díez-Pérez, I.; Tao, N. *J. Am. Chem. Soc.* **2011**, *133* (47), 19189.
(28) Nitzan, A. *Isr. J. Chem.* **2002**, *42*, 163.
(29) Berlin, Y. A.; Ratner, M. A. *Radiat. Phys. Chem.* **2005**, *74* (3−4), 124.
(30) Hihath, J.; Xu, B.; Zhang, P.; Tao, N. *Proc. Natl. Acad. Sci. U. S. A.* **2005**, *102* (47), 16979.
(31) Rubio, G.; Agraït, N.; Vieira, S. *Phys. Rev. Lett.* **1996**, *76* (13), 2302.
(32) Huang, Z.; Chen, F.; Bennett, P. A.; Tao, N. *J. Am. Chem. Soc.* **2007**, *129* (43), 13225.
(33) Noy, A.; Vezenov, D. V.; Kayyem, J. F.; Meade, T. J.; Lieber, C. M. *Chem. Biol.* **1997**, *4* (7), 519.
(34) Meisner, J. S.; Ahn, S.; Aradhya, S. V.; Krikorian, M.; Parameswaran, R.; Steigerwald, M.; Venkataraman, L.; Nuckolls, C. *J. Am. Chem. Soc.* **2012**, *134* (50), 20440.
(35) Bruot, C.; Palma, J. L.; Xiang, L.; Mujica, V.; Ratner, M. A.; Tao, N. *Nat. Commun.* **2015**, *6*, 8032.

DOI: 10.1021/jacs.5b08668
J. Am. Chem. Soc. 2015, 137, 13933−13937